PHYSICAL REVIEW E **67**, 015103(R) (2003)

Universality and double critical end points

J. A. Plascak[1,2] and D. P. Landau[1]
[1]*Center for Simulational Physics, The University of Georgia, Athens, Georgia 30602*
[2]*Departamento de Física, UFMG-ICEx, Caixa Postal 702 30123-970, Belo Horizonte, MG, Brazil*

(Received 23 May 2002; published 24 January 2003)

A double critical end point in the two-dimensional spin-3/2 Blume-Capel model is studied via extensive Monte Carlo simulations. The resultant scaling character of the probability distribution of the mixing scaling operators allows us to locate the double critical end point precisely and also to convincingly show that it indeed belongs to the same universality class as the critical points.

DOI: 10.1103/PhysRevE.67.015103 PACS number(s): 64.60.−i, 02.70.Uu, 05.50.+q, 05.70.Jk

Multicritical phenomena have been the subject of intense study for more than half a century, both experimentally and theoretically. One of the first multicritical points investigated is the tricritical point (TCP), which can be roughly viewed as a point separating a first-order transition line from a second-order transition line (or, by analogy to the critical point, the end of a line of three-phase coexistence, at which the three coexisting phases simultaneously become critical). Tricritical points occur in a variety of systems [1], e.g., ^{3}He-^{4}He mixtures, metamagnets, multicomponent fluid mixtures, etc. Tricritical phenomena are well understood with the tricritical exponents differing from the critical ones, and being equal to the classical exponents for dimensions $d \geqslant 3$. In some cases, however, instead of a TCP, one finds a critical end point (CEP) when a line of second-order phase transitions terminates at a first-order phase boundary delimiting a new noncritical phase. The CEP are common in a variety of physical systems, notably superfluids, binary fluid mixtures, binary alloys, some ferromagnets and ferroelectrics, etc. Recently, an extensive Monte Carlo (MC) simulation [2] provided the first evidence of singular behavior on the first-order transition line close to CEP in a classical binary fluid [3,4].

A more unusual end point, the double critical end point (DCE) [5], occurs where two critical lines end simultaneously at a first-order phase boundary (two distinct critical systems coexist; the name *bicritical end point* is sometimes encountered in the literature). Although, not so ubiquitous as the CEP, double critical end points have been experimentally observed in liquid-liquid-vapor equilibrium in binary and quasibinary systems [6], and there is also some indication of a DCE in the metamagnet $FeBr_2$ [7]. From the theoretical point of view, systems such as the next-nearest-neighbor Ising antiferromagnetic model, the layered metamagnet and the random-field Ising model have been considered as strong candidates to present a DCE since, at least according to mean-field approximations (MFA), they exhibit a splitting of the TCP into a CEP and a DCE [8–10]. It has been recently confirmed, however, that such splitting is an artifact of the MFA and, in fact, does not occur in any of the above models: (i) Monte Carlo renormalization group on the three-dimensional ($d=3$) random-field Ising model shows that the phase transition at weak random field belongs to the same universality class as the zero-temperature transition [11]; (ii) theoretical approaches, based on MC simulations, in the $d=2$ [12] and $d=3$ [13,14] next-nearest-neighbor Ising antiferromagnetic model and layered metamagnets, and also the master equation formalism for the $d=2$ layered metamagnet [15], predict only the existence of a TCP. On the other hand, different behavior between two and three dimensions has been observed in the antiferromagnet spin-1 Blume-Capel (BC) model. The MC simulations provided clear evidence for the decomposition of the TCP into a CEP and a DCE in $d=3$ [16] while in $d=2$, only a fully stable TCP is observed [17]. Apparently, fluctuations in $d=2$ are strong enough to destroy the splitting of the TCP in all of the the above models and in $d=3$, where fluctuations are smaller, only the antiferromagnetic BC spin-1 model [18] exhibits the DCE. In addition, questions regarding its universality class are still unanswered [8,13,14,19].

In this paper, we address the question of the universality at a double critical end point: we consider a generalization of the Blume-Capel model to spin 3/2 and provide the simulation evidence for its universal critical behavior. The Hamiltonian is given [20] by

$$\mathcal{H} = -J\sum_{\langle ij\rangle} S_i S_j + \Delta \sum_{i=1}^{N} S_i^2 - H\sum_{i=1}^{N} S_i , \tag{1}$$

where J is the exchange interaction, Δ is the crystal field anisotropy, H is a uniform external field, $S_i = \pm 1/2, \pm 3/2$, and N is the total number of spins. The phase diagram (based on that for the spin-1 model) is schematically depicted in Fig. 1. In the $H=0$ plane, there is an S surface where two ordered phases with opposite magnetizations coexist. At high temperatures, this surface is separated from the paramagnetic phase by a critical line λ. At low T, S contains two distinct regions: S_3 being the locus of $F_3^{\pm}$ ferromagnetic phases (all spins aligned in the $+3/2$ component coexist with the corresponding spin reversed phase for $\Delta < dJ$ and $T=0$) and S_1 the locus of a generally different $F_1^{\pm}$ ferromagnetic phases (for $\Delta > dJ$ and $T=0$, the phase with all spins aligned in the $+1/2$ component coexists with the spin reversed phase). From $\Delta = dJ$, one has a line of quadruple points π where the above four ordered phases coexist, and which terminates at the double critical end point (at this point two critical phases coexist: $F_3^+ \equiv F_1^+$ and $F_3^- \equiv F_1^-$). By switching on an external uniform field H, one produces two symmetric wings of

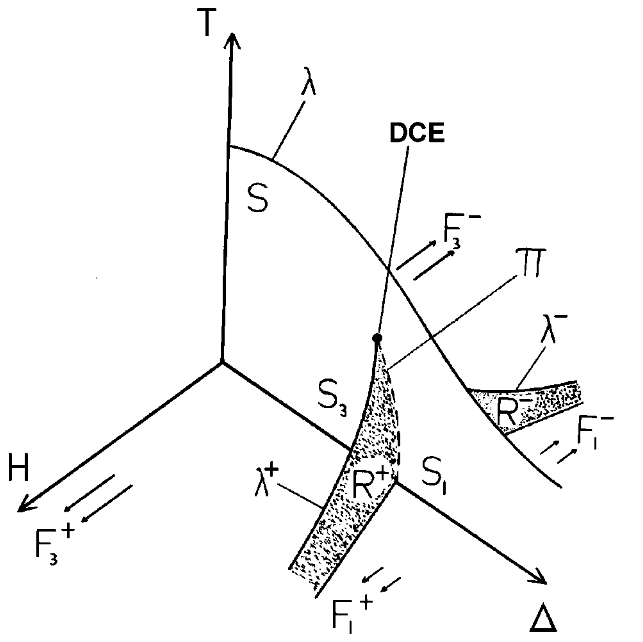

FIG. 1. Schematic phase diagram of the model described by Eq. (1) in the Hamiltonian parameter space. The π line starts at $T=0$, $H=0$, $\Delta=dJ$ and ends at the DCE. For details, see the text.

first-order surfaces $R^{\pm}$, which go to infinity at low temperatures. These wings are limited by $\lambda^{\pm}$ critical lines, respectively, ending at the DCE.

One of the most powerful approaches to the study of magnetic systems by MC simulations is the use of the order parameter distribution function. In addition, MC simulations also provide readily accessible fluctuation spectra of other observables, needed when nonsymmetric phase diagrams are present in field-temperature space, as in this case. It is then worthwhile to define convenient observables as well as to extend the concepts of scale invariance and universality to their distribution probabilities. Due to the invariance of the configurational energy under spin reversal, the π quadruple line, together with the DCE, are immersed in the S surface of Fig. 1. The picture in the $H=0$ plane then resembles the liquid-vapor coexistence curve, with the *double critical* end point at (Δ_d, T_d). This plane has already been explored with different techniques; but controversy about the very nature of this point (if it is critical or tetracritical) precluded studies of its universal behavior [21]. We now know that the lack of symmetry among the four different phases leads to the well-known *mixing* scaling fields [22]: this multicritical point is in fact controlled by three relevant scaling fields τ, g ,h comprising linear combinations of the three single-thermodynamic fields T, Δ, H as

$$\tau=T-T_d+s(\Delta-\Delta_d),$$

$$g=\Delta-\Delta_d+r(T-T_d), \quad h=H(H_d=0), \tag{2}$$

where s and r control the degree of field mixing in the S surface (the special spin reversal symmetry implies $h=H$). As a result, the conjugate scaling operators $\mathcal{E},\mathcal{D},\mathcal{M}$ are also linear combinations of the nearest-neighbor energy density u, the quadrupole q, and magnetization m as

$$\mathcal{E}=\frac{(u-rq)}{1-rs}, \quad \mathcal{D}=\frac{(q-su)}{1-rs}, \quad \mathcal{M}=m, \tag{3}$$

$$u=\frac{1}{N}\sum_{\langle ij\rangle} S_iS_j, \quad q=\frac{1}{N}\sum_{i=1}^{N} S_i^2, \quad m=\frac{1}{N}\sum_{i=1}^{N} S_i. \tag{4}$$

According to finite-size scaling [23] and renormalization group procedures [24], the joint probability distribution $p_L(\mathcal{E},\mathcal{D},\mathcal{M})$ near criticality should obey the following scaling ansatz for sufficiently large system sizes L:

$$p_L(\mathcal{E},D,M)\simeq\Lambda_{\mathcal{E}}^{+}\Lambda_{\mathcal{D}}^{+}\Lambda_{\mathcal{M}}^{+} \times\tilde{p}(\Lambda_{\mathcal{E}}^{+}\delta\mathcal{E},\Lambda_{\mathcal{D}}^{+}\delta\mathcal{D},\Lambda_{\mathcal{M}}^{+}\delta\mathcal{M},\Lambda_{\mathcal{E}}\tau,\Lambda_{\mathcal{D}}g,\Lambda_{\mathcal{M}}h), \tag{5}$$

$$\Lambda_{\mathcal{E}}=a_{\mathcal{E}}L^{d-y_{\mathcal{E}}}, \quad \Lambda_{\mathcal{D}}=a_{\mathcal{D}}L^{d-y_{\mathcal{D}}}, \quad \Lambda_{\mathcal{M}}=a_{\mathcal{M}}L^{d-y_{\mathcal{M}}},$$

where $\Lambda_{\mathcal{E}}\Lambda_{\mathcal{E}}^{+}=\Lambda_{\mathcal{D}}\Lambda_{\mathcal{D}}^{+}=\Lambda_{\mathcal{M}}\Lambda_{\mathcal{M}}^{+}=L^d$, and $\delta\mathcal{E}=\mathcal{E}-\langle\mathcal{E}\rangle_c$, $\delta\mathcal{D}=\mathcal{D}-\langle\mathcal{D}\rangle_c$, $\delta\mathcal{M}=\mathcal{M}-\langle\mathcal{M}\rangle_c$, and c stands for averages taken at criticality and y_i for the eigenvalues. For appropriate choices of the nonuniversal factors $a_{\mathcal{E}}$, $a_{\mathcal{D}}$, and $a_{\mathcal{M}}$, the function $\tilde{p}$ is expected to be universal [25]. Precisely at criticality, one has

$$p_L(\mathcal{E},\mathcal{D},\mathcal{M})\simeq\Lambda_{\mathcal{E}}^{+}\Lambda_{\mathcal{D}}^{+}\Lambda_{\mathcal{M}}^{+}\tilde{p}^{*}(\Lambda_{\mathcal{E}}^{+}\delta\mathcal{E},\Lambda_{\mathcal{D}}^{+}\delta\mathcal{D},\Lambda_{\mathcal{M}}^{+}\delta\mathcal{M}), \tag{6}$$

where $\tilde{p}^{*}(x,y,z)$ is the $\tilde{p}$ function in Eq. (5) for $\tau=g=h=0$. It follows that $\tilde{p}^{*}(x,y,z)$ constitutes a hallmark of a universality class. This distribution will be exploited here. Through extensive Monte Carlo simulations along the first-order line for $d=2$, we will be able not only to determine the universal behavior of the DCE but also to find its precise location in the phase diagram.

In the course of the simulations to determine the π quadrupole line, we studied square $L\times L$ lattices with fully periodic boundary conditions for system sizes of length $8\leqslant L\leqslant 64$ at $H=0$. Following equilibration, runs comprising up to 6×10^6 MCS (Monte Carlo steps per site) were performed using metropolis sequential single spin-flip updates. Histogram reweighting [26] and finite-size scaling techniques were used to precisely locate the first-order transition line by measuring the minima of the fourth-order cumulants of the energy and order parameter, and also the maxima of the specific heat, the linear magnetic susceptibility and quadrupole susceptibility. This approach has proved to be quite efficient and provides good results in studying strong first-order transitions. Figure 2 depicts the phase diagram close to the DCE including the second-order λ boundary. It turns out, however, that not all points along the π line actually identify the coexistence curve itself; but a continuation of it persists in finite-size systems (just a rough estimate of the terminus of the weak first-order line is achieved in this case). To over-

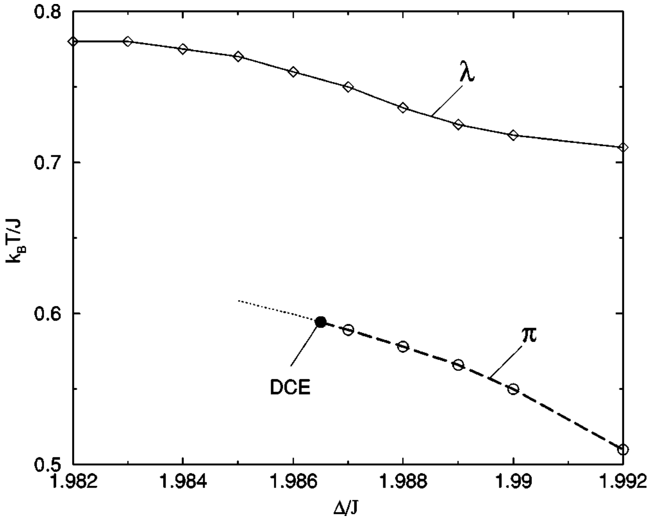

FIG. 2. Portion of the S surface phase diagram of Fig. 1 close to the DCE (in the reduced variables Δ/J and k_BT/J). Diamonds represent the second-order λ phase transition line. Circles give the first-order π transition line (the dashed line is a guide to the eyes). The finite-size extension is given by the dotted line. The filled circle indicates the position of the DCE. Errors do not exceed the symbol sizes.

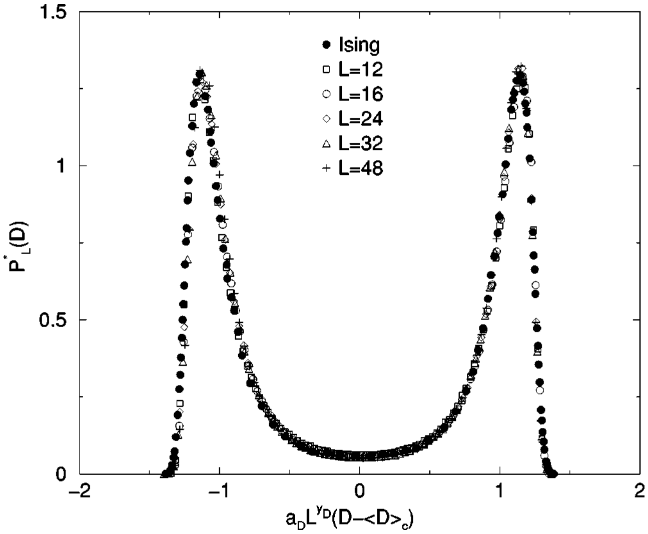

FIG. 3. Scaling operator distribution $\tilde{p}^*(\mathcal{D})$ for several values of L according to the parameters given in the text. Also shown for comparison is the corresponding distribution for the two-dimensional Ising model for $L=32$. All distributions are scaled to unit norm and variance. Statistical errors do not exceed the symbol sizes.

come this difficulty in determining the precise location of the DCE from the previous measurements, the $\tilde{p}^*$ distribution was invoked.

Having obtained the location of the first-order transition line, we made longer runs with 1.2×10^7 MCS for lattices $L\leqslant32$ and 3.0×10^7 MCS for $L=48,64$. During the simulations, the joint probability distribution $p_L(u,q,m)$ was collected in the form of a histogram. This distribution is related to that of the scaling operators given in Eq. (5) through

$$p_L(u,q,m)=\frac{1}{1-rs}p_L(\mathcal{E},\mathcal{D},\mathcal{M}). \tag{7}$$

Formal integration of $p_L(\mathcal{E},\mathcal{D},\mathcal{M})$ over one or more variables provides lower-dimensional distributions, e.g., integrating over $\mathcal{E}$ and $\mathcal{M}$ yields $p_L(\mathcal{D})$. This is the desired distribution since $\mathcal{D}$ is the conjugate scaling operator of the corresponding scaling field g. Choosing the non-universal scale factor $a_{\mathcal{D}}$ in Eqs. (3)–(7) so that, for each system size, the one-dimensional distribution probability $p_L(\mathcal{D})$ as a function of the variable $y=a_{\mathcal{D}}L^{y_{\mathcal{D}}}(\mathcal{D}-\langle\mathcal{D}\rangle_c)$ has unit variance, we are left with only three parameters: the reduced temperature $t=k_BT/J$, the crystal field ratio $\delta=\Delta/J$, and the field mixing parameter s. Thus, by tuning t, δ and s, again with the aid of the histogram reweighting technique, we analyzed the shape of the distribution $\tilde{p}^*_L(\mathcal{D})$ and searched for a symmetric behavior in the y variable. This provides an additional criterion for determining coexisting phases and produces results in close agreement with the procedure described above. Moreover, the great advantage now is that the $\tilde{p}^*_L(\mathcal{D})$ obtained can be mapped to a previously computed distribution presumed to be a member of the same universality class. Figure 3 presents the distribution $\tilde{p}^*_L(\mathcal{D})$, together with the one obtained for the spin-1/2 Ising model at its exact

TABLE I. Parameters for the $\tilde{p}^*(\mathcal{D})$ distribution.

L	t	δ	s
12	0.59650(2)	1.98620(1)	−0.17(1)
16	0.59500(2)	1.98630(1)	−0.18(1)
24	0.59410(2)	1.98646(1)	−0.21(1)
32	0.59390(2)	1.98648(2)	−0.21(1)
48	0.59380(5)	1.98650(2)	−0.21(2)
64	0.59375(5)	1.98652(2)	−0.21(3)

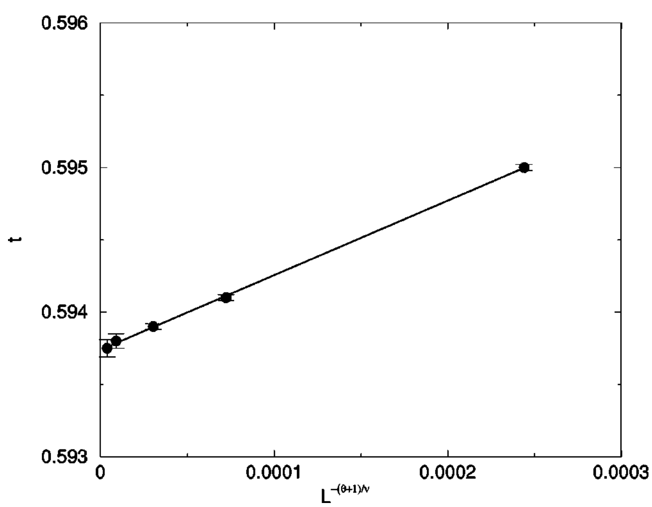

FIG. 4. Reduced temperature t of Table I plotted as a function of $L^{-(\theta+1)/\nu}$ with $\theta=2$ and $\nu=1$ (the exact values for the $d=2$ Ising universality class).

critical temperature. The values for the parameters are given in Table I. The s parameter reaches the value $s = -0.21(3)$, and the parameter $r = -10.0(4)$ is obtained from the measured gradient of the phase boundary at the DCE in Fig. 2. This large value of r reflects the fact that the first-order transition line in the phase diagram is almost vertical (note that the scale for Δ/J is extremely fine in Fig. 2). The dependence of the double critical end point temperature on L is shown in Fig. 4. It has the expected behavior $t(L) = t(\infty) + CL^{-(\theta+1)/\nu}$ [25], where $\nu = 1$ and $\theta = 2$ for $d = 2$ [27], the latter being the correction to scaling exponent. The best estimate for the location of the double critical end point is: $t_d = 0.59374(7)$ and $\delta_d = 1.98647(5)$. From the scaling of the distribution for different finite sizes L as well as from the quite good mapping to the corresponding Ising distribution, one can clearly see that they do indeed belong to the same universality class. The same should hold for the $d = 3$ model with the universality class being that of the three-dimensional Ising model.

Questions regarding possible nonanalyticities in the phase boundary plane (S) close to the DCE can now be easily understood. In fact, the phase boundary for $H = 0$ in Fig. 1 is completely analytic. The absence of singularities, even close to the terminus of the first-order line, is due to the fact that both critical lines λ^+ and λ^- not only are in the same universality class but are symmetric too. This indeed corroborates the prediction suggested by previous scaling arguments [19], where there is a cancellation of the nonanalytic contributions to the phase boundary. However, the scenario should be quite different in a less symmetric context. Even in this case, from our simulations, we argue that the DCE universality class will still be the same as that of the usual critical point, despite the appearance of some singularities in the phase boundary region close to it.

Fruitiful discussions with Shan-Ho Tsai, K. Binder, and W. Figueiredo are kindly acknowledged. This research was supported in part by CNPq and FAPEMIG (Brazilian Agencies) and by NSF Grant No. DMR-0094422.

[1] I.D. Lawrie and S. Sarbach, in *Phase Transitions and Critical Phenomena*, edited by C. Domb and J.L. Lebowitz (Academic, London, 1984), Vol. 9. See also Charles M. Knober and Robert L. Scott, *ibid*.
[2] N.B. Wilding, Phys. Rev. Lett. **78**, 1488 (1997).
[3] M.E. Fisher and P.J. Upton, Phys. Rev. Lett. **65**, 2402 (1990); **65**, 3405 (1990).
[4] M.E. Fisher and M.C. Barbosa, Phys. Rev. B **43**, 11 177 (1991); **43**, 10 635 (1991); M.C. Barbosa, *ibid.* **45**, 5199 (1992).
[5] M.E. Fisher (private communications).
[6] W. Poot and T.W. de Loos, Phys. Chem. Chem. Phys. **1**, 4923 (1999).
[7] K. Katsumata, H. Aruga Katori, S.M. Shapiro, and G. Shirane, Phys. Rev. B **55**, 11 466 (1997); W.P. Wolf, Braz. J. Phys. **30**, 794 (2000).
[8] J.M. Kincaid and E.G.D. Cohen, Phys. Lett., C **22**, 57 (1975).
[9] E. Stryjewski and N. Giordano, Adv. Phys. **26**, 487 (1977).
[10] M. Kaufman, P.E. Klunzinger, and A. Khurana, Phys. Rev. B **34**, 4766 (1986).
[11] M. Itakura, Phys. Rev. B **64**, 012415 (2001); D.P. Belanger, Braz. J. Phys. **30**, 682 (2000).
[12] D.P. Landau and R.H. Swendsen, Phys. Rev. Lett. **46**, 1437 (1981); Phys. Rev. B **33**, 7700 (1986).
[13] H.J. Herrmann and D.P. Landau, Phys. Rev. B **48**, 239 (1993).
[14] M. Zukovic and T. Idogaki, Phys. Rev. B **61**, 50 (2000).
[15] M. Santos and W. Figueiredo, Phys. Rev. B **58**, 9321 (1998).
[16] Y.-L. Wang and J.D. Kimel, J. Appl. Phys. **69**, 6176 (1991).
[17] J.D. Kimel, S. Black, P. Carter, and Y.-L. Wang, Phys. Rev. B **35**, 3347 (1987).
[18] H.J. Herrmann, E.B. Rasmussen, and D.P. Landau, J. Appl. Phys. **53**, 7994 (1982).
[19] E.L. de Santa Helena and Marcia C. Barbosa, Physica A **208**, 479 (1994).
[20] M. Blume, Phys. Rev. **141**, 517 (1966); H.W. Capel, Physica (Amsterdam) **32**, 966 (1966).
[21] J.A. Plascak and D.P. Landau, in *Computer Simulation Studies in Condensed Matter Physics XIII*, edited by D. P. Landau, S. P. Lewis, and H. -B. Shuttler (Springer, Berlin, 2000), and references therein.
[22] F.J. Wegner, Phys. Rev. B **5**, 4529 (1972).
[23] A.D. Bruce and N.B. Wilding, Phys. Rev. Lett. **68**, 193 (1992); J. Phys.: Condens. Matter **4**, 3087 (1992).
[24] A.D. Bruce, J. Phys.: Condens. Matter **14**, 3667 (1981).
[25] K. Binder, Z. Phys. B: Condens. Matter **43**, 119 (1981).
[26] A.M. Ferrenberg and R.H. Swendsen, Phys. Rev. Lett. **61**, 2635 (1988).
[27] P. Calabrese, M. Caselle, A. Celi, A. Pelisseto, and E. Vicari, J. Phys. A **33**, 8155 (2000); J. Salas and A. Sokal, J. Stat. Phys. **98**, 551 (2000); S.L.A. de Queiroz, J. Phys. A **33**, 721 (2000).